Supporting Information

Friction in Carborane-Based Molecular Rotors Driven by Gas Flow or Electric Field: Classical Molecular Dynamics

Alexandr Prokop,[a,b] Jaroslav Vacek,[a,b]* and Josef Michl[a,b]*

[a]*Institute of Organic Chemistry and Biochemistry, Czech Academy of Sciences, Flemingovo nám. 2, Praha 6, Czech Republic*

[b]*Department of Chemistry and Biochemistry, University of Colorado, Boulder, CO 80309-0215, U.S.A.*

Table of Contents

The TINK Program and UFF Force Field. Molecular polarizability, radiative losses due to charge acceleration (entirely negligible in our case), and all quantum effects were neglected. The program solves Newton's equations of motion for molecular systems of asize limited only by computer memory, containing atoms of any elements. Atoms are allowed to enter and exit, and arbitrary time-dependent electric fields can be imposed from the outside.

The atomic charges within the whole assembly are calculated at a single optimized geometry with a particular orientation of the rotor dipole. This has the effect of biasing the charge distribution in the rest of the assembly. This is unfortunate in principle but a comparison with a few dynamics runs performed with multi-configurationally averaged charges showed that it has very little effect in practice since the rotational energy of the propellers stays above these barriers in any event (Figure S1).

Charges on rare gas atoms were set to zero. Those on the tetracoordinate B^- and N^+ atoms located at the tips of the propeller blades and on the negatively charged *closo*-borate anions **2** and **3** were obtained from a MP2/6-31G** calculations for model systems ($BF_2Me_2^-$, NMe_4^+, 1,12-dimethyl-2,7,3,8,3,9,5,10,6,11-pentakis(1,3-butadiene-1,4-diyl)monocarba-*closo*-dodecaborate anion and 1,14-dimethyl-2,8,4,10,6,12-tris(1,3-butadiene-1,4-diyl)monocarba-*closo*-tetradecaborate anion, respectively) using the ESP electrostatic potential fitting procedure.[1] The ab initio calculations used the Gaussian98 program.[2]

Modified Force Field for Carboranes. Preliminary tests indicated that some properties of the original UFF force field[3,4] were unsatisfactory for carboranes, and we used the force field parameters recently derived for their carbon and boron atoms by comparison with results of MP2/6-31G** calculations.[5] These parameters were adjusted to reproduce the equilibrium geometry and

the rigidity of the carborane cage and are listed in Table S1.

Rotor Structures. The hub of each rotor is represented by one of the following: the 10-vertex 1,10-dicarba-*closo*-decaborane ($C_2B_8H_{10}$, **1**), the 12-vertex 1-carba-*closo*-dodecaborate anion ($CB_{11}H_{12}^-$, **2**), and the 14-vertex 1-carba-*closo*-tetradecaborate anion ($CB_{13}H_{14}^-$, **3**) or 1,14-dicarba-*closo*-tetradecaborane ($C_2B_{12}H_{14}$, **4**). The dicarbaboranes are electroneutral and the monocarbaborate anions have a delocalized negative charge. There are two or four blades in **1**, five in **2**, and two, three or six in **3** and **4**. Each divalent substituent **a** - **d** is attached to boron atoms at two adjacent vertices of the deltahedral hub, one at each of the two equatorial polygons ("belts") of boron atoms present. The remaining equatorial borons, if any, carry hydrogens. The axial positions of the resulting two- to six-bladed hubs are occupied by two carbons in the neutral *para*-dicarbaboranes **1** and **4**, and by one carbon and one boron in the anionic monocarborates **2** and **3**. They are connected to [*n*]staffane axles that permit attachment to the grid via terminal nitrile groups..

The double grid segment consists of two parallel layers of four squares (2 × 9 connectors and 2 × 12 horizontal rods) with the propeller axle in the center. The exo-oriented axial positions of all Rh_2^{4+} connectors are occupied by acetonitrile ligands. The endo-oriented positions of the eight Rh_2^{4+} connectors remaining in each layer were used to connect the two layers with 8 vertical rods consisting of a 12-vertex *p*-carborane carrying two nitrile terminated [*m*]staffanes in antipodal positions (Figure 2 in the main text).

The response of three different scaffolds marked **A** ($n = 6$, $m = 2$), **B** ($n = 8$, $m = 2$) and **C** ($n = 8$, $m = 3$) to gas flow was tested initially. The scaffold **A** with the smallest openings was unsatisfactory. The propeller in the molecular rotor **A10a4** rotated slowly and in **A12a5** it did not rotate at all. The grid **B** with next larger openings gave only slightly better results and the propeller

in **B12a5** rotated slowly in Ne. The more spacious grid **C** was found the most appropriate and was utilized in all subsequent calculations.

Molecular Dynamics with Gas Flow. The geometry of each assembly was first optimized. The rare gas atoms were created at random positions in a volume located at least 90 - 100 Å upstream of the propeller and were assigned a 10 K Maxwellian distribution of velocity vectors, to which the flow velocity vector was added. They approached the grid along the *z* axis, perpendicular to the grid surface and their motion was followed until they were at least 30 Å below the grid, whereupon they were annihilated. For each atom that was removed at the bottom one was created on the top, such that the total number of particles was conserved.

All atoms moved freely, except that several constraints were introduced to simulate the effect of a holder on which the grid would be mounted in reality, such as a metal mesh or a perforated membrane. The constraints prevented the molecular rotor from being swept away by the gas stream. (i) The position of the Rh atom to which the propeller was attached was fixed in space and represented the origin of the coordinate system. (ii) The twenty-four bridgehead hydrogen atoms at the periphery of the grid were allowed to move only in the *xy* plane, perpendicular to the gas flow direction.

In some simulations the motion of helium atoms was constrained to a square tube with an axis parallel to *z* and a 53 Å × 53 Å or 73 Å × 73 Å cross-section in the *xy* plane. The tube reached at least 20 Å above the grid and had perfectly reflecting walls. By returning atoms that would otherwise escape from the interaction region, the tube simulated the fact that in a realistic experimental situation gas atoms scattered by neighboring propellers would also enter the region of interest.

We have also studied the behavior of solitary propellers not mounted on any molecular grid. In these simulations we could examine the effect of the propeller geometry (the number of blades, their inclination against the direction of the gas flow and the presence of charged groups at the tips of propeller blades) on propeller performance without intervention of a molecular grid. During these simulations the terminal atoms of the propeller axle were kept fixed and the rotor axis was oriented along the *z* axis.

Each run started with the molecular rotor at 300 K and lasted for 500 - 1000 ps. After some testing the integration step was set to 1.7 fs. In order to minimize the time necessary for each run we used relatively high gas densities and flow velocities. Most of the MD runs used a helium gas number density of 2 atoms/nm^3 (~2.4 atm in the ideal gas approximation), and a flow velocity of 1841 ms^{-1}. These parameters represent conditions attainable in a laminar stream of gas near the nozzle of a standard supersonic jet with a room temperature gas reservoir. The simulation setup is depicted in Figure 3 in the main text.

Molecular Dynamics with Rotating Electric Field. When an external electric field of strength E directed in the xy plane and rotating at frequency ν was applied to drive the rotational motion of the dipolar molecular propeller, the MD constraints on the molecular dynamics, the starting temperature and the length of simulation were kept as close as possible to those employed in the calculations with streaming He. Frequencies ν ranged from 3 to 160 GHz, and the field strength E varied between 108 and 11961 kVcm^{-1}.

Properties Monitored. Several system characteristics were evaluated continuously. Pointed brackets indicate time averages. The quantities calculated over the whole duration of a run are unprimed and those computed only over a steady state period of smooth rotation are primed.

Ensemble averages are indicated with a bar.

Instantaneous gas temperature T(g) was evaluated in a volume reaching 50 Å above [$T(\mathrm{g})^{\mathrm{above}}$] and 50 below [$T(\mathrm{g})^{\mathrm{below}}$] the center of the propeller, using

$$T(\mathrm{g}) = (m_{\mathrm{g}}/3n_{\mathrm{g}}k) \sum_{i\varepsilon\{g\}} | \mathrm{v}^i - \bar{\mathrm{v}}_{\mathrm{z}} |^2 \tag{S1}$$

where m_{g} is the mass and n_{g} is the number of the gas atoms in the volume, k is the Boltzmann constant, v^i is the velocity vector of the i-th gas atom, v_z^i is its z component, and {g} is the set of n_{g} gas atoms above or below the center of the propeller. The instantaneous gas flow energy density above and below the propeller is

$$E_{\mathrm{trans}}^{\mathrm{above}}(\mathrm{g},t) = (1/2)m\sum_{i\varepsilon\{g\}} (\mathrm{v}_z^i)^2 / V^{\mathrm{above}} \tag{S2}$$

$$E_{\mathrm{trans}}^{\mathrm{below}}(\mathrm{g},t) = (1/2)m\sum (\mathrm{v}_z^i)^2 / V^{\mathrm{below}}$$

where V^{above} is the volume above and V^{below} the volume below the system and t is time. The time-averaged gas-flow energy density is

$$E_{\mathrm{trans}}(\mathrm{g},r) = (1/2)\langle d_{\mathrm{g}}\rangle m_{\mathrm{g}}\langle \mathrm{v}_z\rangle^2 \tag{S3}$$

The gas number density $d_{\mathrm{g}}(r)$ and the z component of gas velocity $\langle \mathrm{v}_z(r)\rangle$ were evaluated in

a volume V of 2Å × 2 Å × 2 Å centered at r,

$$<d_g(r)> = <n_g(r)/V> \tag{S4}$$

where $n_g(r)$ is the number of gas atoms in the volume V. The average z component of the gas velocity vector is approximated by

$$\overline{v}_z = \sum_{i\varepsilon\{g\}} v_z^i / n_g \tag{S5}$$

where n_g is the total number of gas atoms in the volume. This expression becomes exact in the limit of large n_g.

The z component of the instantaneous torque on the propeller induced by the flowing gas $N^D_{z,gas}$ is calculated as

$$N^D_{z,gas} = \sum_i^n \sum_j^N (F_x^{ij} y_j - F_y^{ij} x_j) \tag{S6}$$

where F_x^{ij} *and* F_y^{ij} are components of force between gas particle i and propeller atom j in xy plane perpendicular to direction of flowing gas. N is the number of atoms forming the propeller and n is the number of gas particles instantaneously found within the interaction cutoff distance of the propeller.

The propeller angular velocity is

$$\bar{\omega}_z = L_z(p)/I_z \tag{S7}$$

where

$$L_z = \sum_{i\varepsilon\{p\}} m_i \,|\, v_t^i \,|\,|\, r_{xy}^i \,| \tag{S8}$$

is its angular momentum, v_t^i is the tangential velocity vector, m^i is the mass of propeller atom *i*, $|r_{xy}{}^i|$ is a projection of the distance of atom *i* from the rotational axis into a plane perpendicular to that axis, $I_z = \sum_{i\{p\}} m^i \,|r_{xy}{}^i|^2$ is its moment of inertia, and {p} is the set of propeller atoms. The temperature equivalent T_{eq}(p) of the rotational kinetic energy is

$$T_{eq}\,(\mathrm{p}) = (1/k) \sum_{i\varepsilon\{p\}} m^i\,(v_t^i)^2 = (1/k)\, I_z\, \bar{\omega}_z^2 \tag{S9}$$

The temperature in the instantaneous rotating reference frame is

$$T_{rot}\,(\mathrm{p}) = (1/n_p k) \sum_{i\varepsilon\{p\}} m^i\,(\nu_t^i - \bar{\nu}_t^i)^2 = (1/n_p k) \sum_{i\varepsilon\{p\}} I_z^i\,(\omega_z^i - \bar{\omega}_z^i)^2 \tag{S10}$$

The overall propeller temperature is

$$T_{tot}\,(\mathrm{p}) = (1/3n_p k) \sum_{i\varepsilon\{p\}} m^i\,(\nu^i - \bar{\nu}_t^i)^2 \tag{S11}$$

Here, m^i is the mass of atom i, I_z^i is the moment of inertia of atom i, ω_z^i and v_t^i are the angular and tangential velocity vectors of atom i, and $|v_t^i|$ is calculated from the overall angular velocity $\bar{\omega}_z$,

$$|\bar{v}_t^i| = \bar{\omega}_z \, |r_{xy}{}^i| \tag{S12}$$

In determining T_{rot}(p), only the angular contribution of the motion of each atom is counted (a single degree of freedom per propeller atom). In determining the overall temperature T_{tot}(p), all motions of its atoms in the rotating frame are counted. The temperature equivalent T_{fluc}(p) of the kinetic energy of fluctuation of the propeller overall rotational motion is

$$T_{fluc}(\mathrm{p}) = (1/k)\, I_z(\bar{\omega}_z - \langle\omega_z\rangle)^2 \tag{S13}$$

Since one atom had a fixed position and 24 were allowed to move only in *xy* plane, the number of degrees of freedom taken into calculation of the overall grid temperature T_{tot}(gr) was $3n_{gr} - 27$, where n_{gr} is the number of atoms in the grid.

In the simulations in rotating electric field, additional characteristics related to the interaction of the rotor dipole moment μ with the electric field vector E were monitored: average lag angle $\langle\alpha\rangle$ of the rotor behind the field and average polarization $\cos\langle\alpha\rangle$. The probability of skipping a turn of the field $\langle a\rangle$ was determined as:

$$a = \alpha_{tot}/2\pi n \tag{S14}$$

where α_{tot} is total lag angle of propeller after n turns of the field.

The definitions of the probabilities of forward and backward skipping in the model based on thermally activated hopping within a potential defined in a system of axes rotating at the angular frequency ω are

$$p = 10^{13}\exp(-\Delta U/kT) \quad \text{(S15)}$$

$$p' = 10^{13}\exp(-\Delta U'/kT) \quad \text{(S16)}$$

The potential changes associated with skipping (ΔU) or gaining ($\Delta U'$) a turn are

$$\Delta U = 2[E\mu\cos\langle\alpha\rangle + \eta_a(\nu)\omega(\pi/2 - \langle\alpha\rangle)] \quad \text{(S17)}$$

$$\Delta U' = 2[E\mu\cos\langle\alpha\rangle + \eta_a(\nu)\omega(3\pi/2 - \langle\alpha\rangle)] \quad \text{(S18)}$$

where $\langle\alpha\rangle$ represents the mean value of the lag angle α. To obtain a value of $\eta_a(\nu)$, we fitted $a(E,\nu,T)$ using an adaptive nonlinear least-squares algorithm.[6]

Figure S2 provides an illustration of the distribution of gas atom speeds as a function of position within a molecular rotor, and Figure S3 shows examples of the time development of gas density at three distances from the propeller.

Table S2 collects results for rotor performance in a stream of gas, and Tables S3 and S4, in rotating electric field. Table S5 provides an example of the gradual heating of the molecular rotor in rotating electric field.

Table S1. UFF parameters of C and B atoms in carboranes.[5]

Atom type [a]	Covalent radius (Å)	Valence angle	Effective charge *Z**
C_*B*	0.88	93.071	1.065
B_*B*	0.82	120.571	1.04

[a] The second letter stands for class of carborane. For more detail, see Ref. 1.

Table S2. Examples of performance of molecular propellers in a stream of gas.[a]

Rotor	Gas	ρ^{gas}/nm^3	v_z/ms^{-1}	t_{tot}/ps	$\langle v^{\wedge}\rangle$/GHz	$\langle v\rangle$/GHz	τ_0/ps	τ/τ'	R/ps^{-1}	$\langle N^D_{z,gas}\rangle$	T_{eq}(p)	T_{rot}(p)	T_{tot}(p)	T_{fluc}(p)
C10a4	He	2.0	1841	689.64	2.92	10.40	54	0.26	0.07	0.09	384	326	325	360
C10a4	He	2.0	2250	689.64	11.89	19.14	78	0.28	0.08	0.12	932	487	483	547
C10a4	He	1.0	2598	689.64	7.00	19.16	48	0.06	0.09	0.03	726	572	566	541
C10a4	He	3.0	1841	689.64	3.62	9.83	78	0.29	0.07	0.11	398	337	335	362
C10a4	He	4.0	1841	555.85	6.71	14.51	111	0.20	0.07	0.15	453	324	321	342
C10a4	He	1.5	2250	689.64	2.71	18.82	62	0.09	0.11	0.21	542	454	449	517
C10c4	He	2.0	1841	689.64	5.32	8.72	57	0.24	0.04	0.14	423	322	317	254
C10c4	He	2.0	2250	689.64	7.72	13.81	35	0.16	0.05	0.23	824	470	466	465
C10c4	He	2.0	2598	689.64	16.16	17.32	59	0.42	0.05	0.16	2170	633	626	602
C10c4	He	1.0	2598	689.64	12.41	17.76	135	0.62	0.07	0.20	1772	581	577	845
C10c4	He	1.0	1841	689.64	4.77	17.19	35	0.17	0.08	0.17	581	298	294	465
C10c4	He	1.5	1841	689.64	6.37	15.60	55	0.13	0.06	0.08	564	321	316	333
C10c4	He	1.5	2250	689.64	11.46	18.46	62	0.17	0.06	0.22	1341	469	463	563
C10c4	He	3.0	1841	689.64	4.91	8.31	47	0.34	0.04	0.21	474	330	325	333
C12a5	He	2.0	1841	689.64	5.83	15.82	50	0.18	0.08	0.29	476	343	341	355
C12a5	He	2.0	2250	689.64	11.49	23.83	41	0.26	0.09	0.14	1004	457	454	529
C12a5	He	2.0	2598	689.64	9.03	15.85	41	0.35	0.08	0.25	1080	585	586	788
C12a5	He	3.0	1841	689.64	4.60	10.00	38	0.43	0.06	0.25	404	326	325	329
C12a5	Ne	1.0	1841	224.82	1.39	4.54	90	0.10	0.05	1.43	1120	1125	1117	1093
C12c5	He	2.0	1841	689.64	8.55	24.39	35	0.04	0.04	0.23	1101	283	278	543
C12c5	He	2.0	2250	689.64	20.78	23.43	53	0.22	0.04	0.12	3841	421	415	512
C12c5	He	2.0	2598	682.74	22.60	22.58	35	0.20	0.05	0.20	4556	625	619	609
C12c5	He	2.0	2598	689.64	25.96	28.20	95	0.19	0.05	0.13	6069	554	549	867
C12c5	He	2.0	2911	541.37	26.43	27.25	34	0.92	0.05	0.22	6180	801	796	761
C12c5	He	1.0	1841	689.64	10.19	17.98	120	0.18	0.05	0.15	1238	364	360	418
C12c5	He	1.0	2598	689.64	24.83	33.07	35	0.17	0.06	0.24	5604	620	617	772

C12c5	He	1.0	2911	689.64	27.37	30.08	59	0.20	0.06	0.13	6948	788	785	980
C12c5	He	1.0	3188	689.64	30.08	37.54	84	0.26	0.07	0.17	5604	620	617	772
C12c5	He	1.5	1841	689.64	10.03	12.84	20	0.07	0.04	0.26	1149	366	364	363
C12c5	He	1.5	2250	689.64	17.51	27.69	51	0.20	0.08	1.06	3248	494	491	884
C12c5	He	3.0	1841	409.65	9.46	13.60	63	0.24	0.04	0.34	921	341	340	356
C12c5	He	4.0	1841	689.64	13.94	15.01	22	0.45	0.03	0.12	1782	354	353	375
C12c5	Ne	2.0	1841	181.40	19.26	22.22	26	0.13	0.07	0.36	4422	1132	1132	1503
C14a6	He	2.0	2250	689.64	3.81	8.07	71	0.36	0.05	0.10	447	448	445	381
C14a6	He	2.0	2598	689.64	6.21	12.37	72	0.24	0.06	0.10	864	653	647	682
C14a6	He	3.0	1841	689.64	3.18	9.14	78	0.19	0.05	0.24	323	338	334	276

[a] ρ^{gas} is the number density of incoming gas atoms, t_{tot} is the total simulation time, $\langle \nu' \rangle$ is the time-averaged rotor frequency over the whole simulation, $\langle \nu \rangle$ is the time-averaged frequency over steady state rotational part, τ_0 is the initial period of irregular rotation, τ/τ' is the fraction of the average rotational period computed over steady state relative to the rotational period computed over whole simulation, R is the RMS fluctuation of the rotational frequency, $\langle N^D_{gas} \rangle$ is the time-averaged gas-induced torque on the propeller, and the various temperatures T are defined in equations (S9) - (S13).

Table S3. Examples of **C12a5** performance in rotating electric field.[a]

Run	n	m	t_{tot} (ps)	E(kV/cm)	ν (GHz)	a	a'	$\langle \nu_{rot} \rangle$ (GHz)	<sinα>	<cosα>	T_{rot}(p)	T_{tot}	<α>	<δα>
1	3.40	1	1042.7	677	3.25	0.249	0.550	2.446	0.156	0.523	308	297	5.866	2.053
2	3.40	2	1042.7	434	3.25	0.604	0.590	1.289	0.217	0.309	314	305	8.017	4.849
3	3.40	3	1042.7	368	3.25	0.797	0.708	0.660	0.325	0.124	307	300	1.271	4.506
4	6.05	6	618.8	173	9.75	1.038	0.958	-0.372	0.180	0.056	310	305	18.211	10.985
5	10.19	10	1042.7	434	9.75	1.013	1.044	-0.130	0.213	0.252	308	302	33.426	18.843
6	10.19	8	1042.7	564	9.75	0.739	0.744	2.552	0.264	0.324	320	312	23.822	13.122
7	10.19	0	1042.7	1410	9.75	0.004	0.008	9.735	0.188	0.751	313	300	0.253	0.709
8	10.19	0	1042.7	1128	9.75	0.004	0.008	9.737	0.164	0.615	311	297	0.243	0.935
9	20.38	0	1042.7	1692	19.5	0.011	0.006	19.337	0.256	0.657	310	298	0.379	0.815
10	20.38	6	1042.7	1410	19.5	0.295	0.196	13.782	0.215	0.273	318	307	12.555	11.159
11	20.38	11	1042.7	1128	19.5	0.544	0.656	8.917	0.218	0.177	312	303	41.981	22.019
12	20.38	12	1042.7	998	19.5	0.587	0.854	8.068	0.245	0.359	316	307	54.687	21.856
13	20.38	13	1042.7	434	19.5	0.648	0.646	6.887	0.264	0.094	319	310	41.395	21.637
14	20.38	18	1042.7	368	19.5	0.891	0.896	2.140	0.177	0.039	315	308	57.351	31.712
15	20.38	20	1042.7	303	19.5	0.995	0.988	0.104	0.136	0.066	315	309	63.239	36.828
16	40.77	37	1042.7	998	39	0.917	0.944	3.246	0.064	-0.089	306	302	120.931	68.935
17	40.77	1	1042.7	2495	39	0.025	0.050	38.140	0.227	0.726	313	306	6.447	0.893
18	40.77	9	1042.7	2695	39	0.215	0.403	30.686	0.186	0.532	307	304	51.592	12.529
19	40.77	0	1042.7	2894	39	0.003	0.003	38.979	0.227	0.684	313	309	0.328	0.84
20	40.77	1	1042.7	3094	39	0.031	0.050	37.875	0.178	0.704	305	303	6.430	1.252
21	40.77	0	1042.7	3294	39	0.002	0.002	39.021	0.196	0.681	316	308	0.248	0.881
22	81.54	80	1042.7	1692	78	0.978	0.982	1.749	0.016	-0.008	311	305	251.457	146.384
23	81.54	43	1042.7	3992	78	0.525	0.658	37.171	0.072	-0.023	331	321	168.582	84.408
24	81.54	2	1042.7	7586	78	0.026	0.050	76.181	0.212	0.899	316	313	12.718	0.786
25	163.07	3	1042.7	9166	156	0.019	0.037	153.411	0.390	0.829	341	332	18.991	1.898
26	163.07	5	1042.7	8367	156	0.032	0.060	151.407	0.387	0.742	340	333	30.923	4.245
27	163.07	87	1042.7	5572	156	0.534	0.562	72.925	0.027	-0.043	347	338	287.806	147.442
28	163.07	162	1042.7	1974	156	0.995	0.992	0.811	0.002	0.005	320	314	508.382	295.911

[a] n is the number of field turns, m is the number of turns skipped by the rotor, t_{tot} is the simulation time, E is the field strength, ν is the field frequency, $\langle \nu_{rot} \rangle$ is the average rotor frequency, a is the mean lag per turn, a' is the time-averaged lag per turn, T_{rot}(p) is the rotor temperature, T_{tot} is the overall temperature of the system, $\langle \alpha \rangle$ is the time-averaged lag angle, and $\langle \delta\alpha \rangle$ is the lag angle rms fluctuation.

Table S4. Examples of **C12c5** performance in rotating electric field.[a]

Run	n	m	t_{tot} (ps)	E (kV/cm)	ν (GHz)	a	a'	$\langle\nu_{rot}\rangle$ (GHz)	$\langle\sin\alpha\rangle$	$\langle\cos\alpha\rangle$	T_{rot}(p)	T_{tot}	$\langle\alpha\rangle$	$\langle\delta\alpha\rangle$
1	163.07	12	1042.7	11162	156	0.075	0.141	144.72	0.467	0.65	450	385	72.273	13.099
2	163.07	14	1042.7	10363	156	0.086	0.154	142.947	0.447	0.544	510	419	78.856	16.949
3	163.07	39	1042.7	9565	156	0.241	0.402	118.726	0.411	0.419	418	373	205.870	66.115
4	163.07	53	1042.7	8766	156	0.326	0.533	105.429	0.384	0.393	393	356	273.236	96.593
5	163.07	54	1042.7	7968	156	0.332	0.427	104.525	0.311	0.193	409	358	218.481	73.497
6	163.07	125	1042.7	7169	156	0.765	0.795	36.827	0.054	0.027	381	342	407.132	225.516
7	163.07	122	1042.7	6371	156	0.746	0.816	39.698	0.062	0.023	376	347	417.980	222.906
8	163.07	134	1042.7	5572	156	0.825	0.835	27.434	0.061	0.017	369	333	427.798	239.553
9	163.07	147	1042.7	4774	156	0.902	0.900	15.344	0.031	-0.003	356	332	460.859	267.986
10	163.07	150	1042.7	3975	156	0.919	0.926	12.653	0.043	0.024	350	326	474.384	269.860
11	163.07	162	1042.7	1974	156	0.993	1.002	1.160	-0.002	-0.002	328	307	513.359	292.572
12	81.54	7	1042.7	8384	78	0.089	0.080	71.205	0.544	0.608	377	352	20.524	4.671
13	81.54	31	1042.7	7586	78	0.382	0.587	48.359	0.28	0.273	353	314	150.364	59.913
14	81.54	73	1042.7	6388	78	0.894	0.904	8.314	0.034	-0.030	340	313	231.666	129.995
15	81.54	76	1042.7	5989	78	0.936	0.926	5.026	0.018	-0.05	328	306	237.074	136.271
16	81.54	79	1042.7	5190	78	0.968	0.979	2.533	0.022	-0.025	325	301	250.782	143.440
17	81.54	80	1042.7	3992	78	0.984	0.985	1.270	0.028	-0.014	320	312	252.343	145.789
18	40.77	36	1042.7	3294	39	0.885	0.964	4.513	0.024	-0.067	310	304	123.422	72.706
19	40.77	8	1042.7	2894	39	0.189	0.122	31.703	0.319	0.256	309	305	15.654	7.522
20	30.26	29	774.0	2495	39	0.959	0.963	1.603	-0.002	-0.089	303	302	91.585	52.916
21	40.77	37	1042.7	1896	39	0.897	0.880	4.011	0.011	-0.056	318	305	112.71	68.824
22	20.38	1	1042.7	1692	19.5	0.044	0.044	18.681	-0.019	0.088	325	299	2.843	4.164
23	17.14	3	877.0	1410	19.5	0.173	0.339	16.17	0.148	0.004	320	304	18.252	5.169
24	20.38	19	1042.7	698	19.5	0.940	0.923	1.166	0.054	-0.081	312	310	59.127	34.936
25	10.19	8	1042.7	902	9.75	0.802	0.947	1.933	0.264	-0.051	310	301	30.33	16.385
26	3.40	0	1042.7	529	3.25	0.009	-0.033	3.229	0.102	0.267	303	283	-0.354	1.713

[a] n is the number of field turns, m is the number of turns skipped by the rotor, t_{tot} is the simulation time, E is the field strength, v is the field frequency, $\langle v_{rot}\rangle$ is the

average rotor frequency, a is the mean lag per turn, a' is the time-averaged lag per turn, $T_{rot}(p)$ is the rotor temperature, T_{tot} is the overall temperature of the system, $<\alpha>$ is the time-averaged lag angle, and $<\delta\alpha>$ is the lag angle rms fluctuation.

Table S5. Heating rate dT_{tot}/dt (K/ns) of molecular propellers mounted on grid **C** in rotating electric field.

Rotor	ν (GHz)					
	3	10	20	40	80	150
C12a5	145	147	150	149	157	172
C12c5	300	145	148	148	160	194

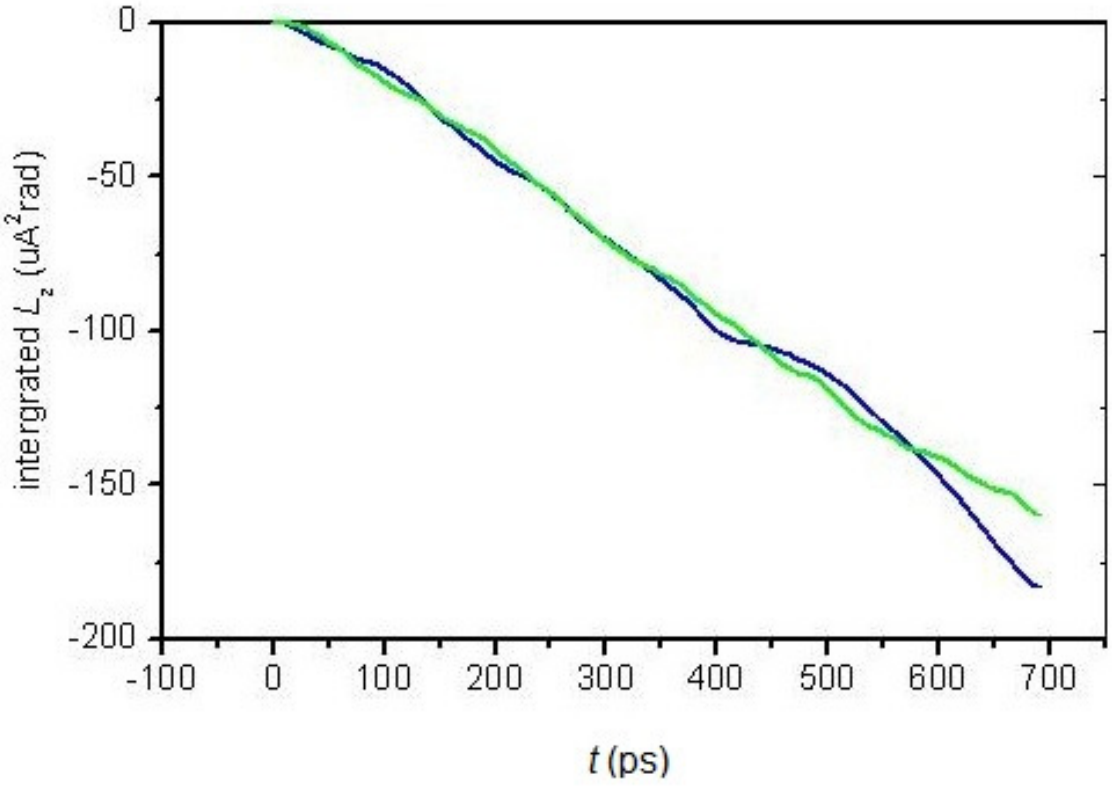

Figure S1. Comparison of molecular dynamics results with and without averaged charges on the molecular grid.

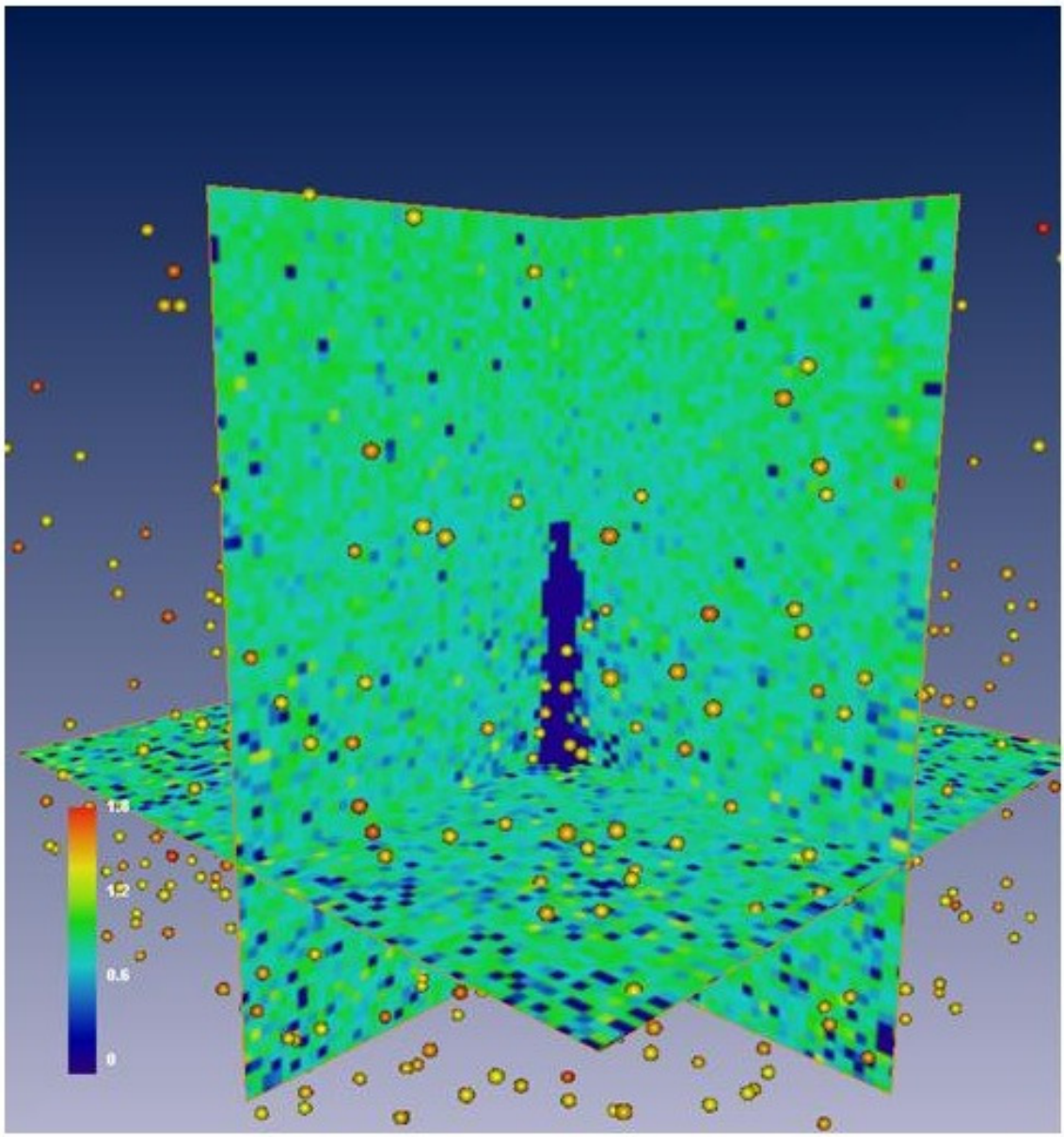

Figure S2. Color (see scale bar) indicates the absolute value of the *z* (vertical) component of the time-averaged velocity of He gas arriving from above, in units of 1841 ms^{-1}, measured at various locations within a 80 Å × 80 Å × 80 Å box centered at the upper Rh atom above the propeller.

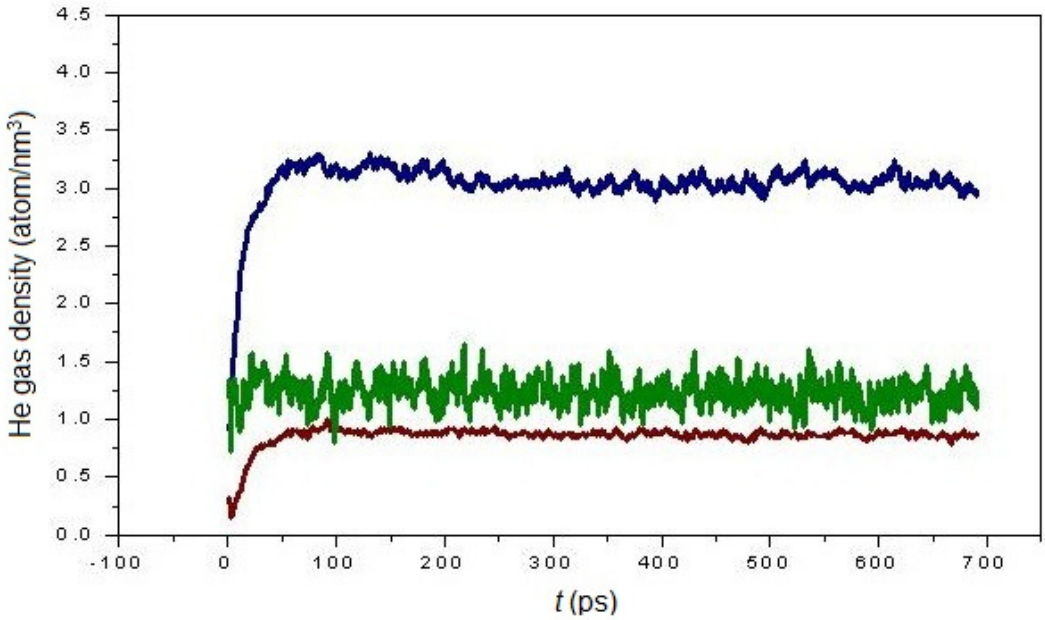

Figure S3. Time evolution of He gas density calculated 50 Å above (blue) and 50 Å below (purple) the propeller, and in its proximity (green).

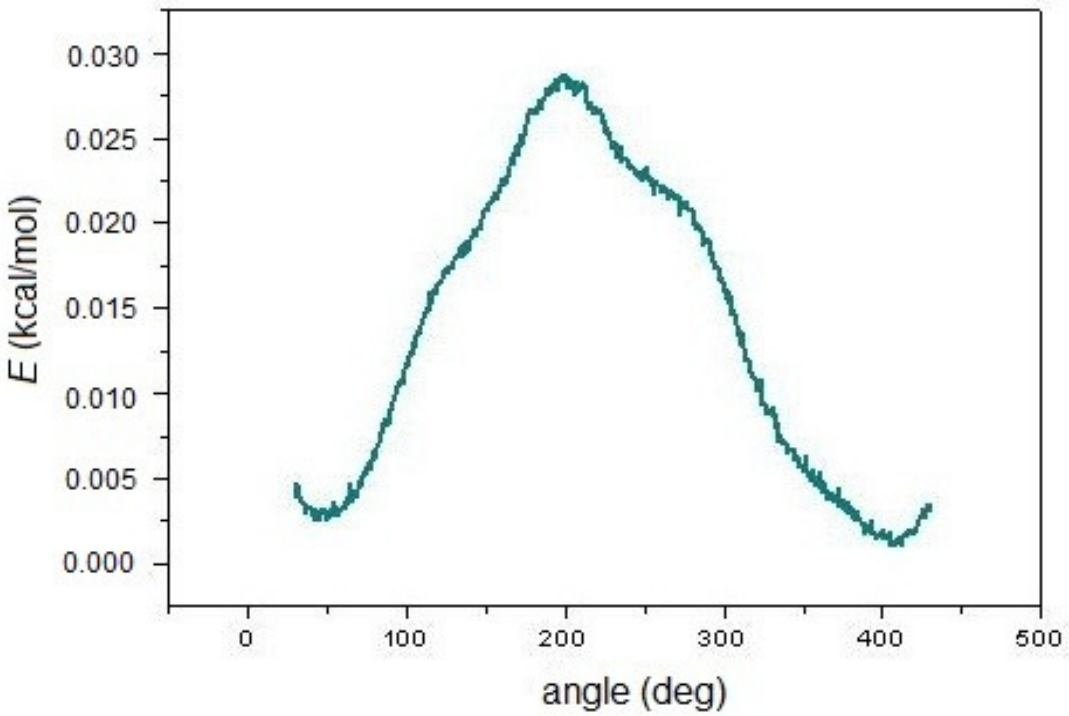

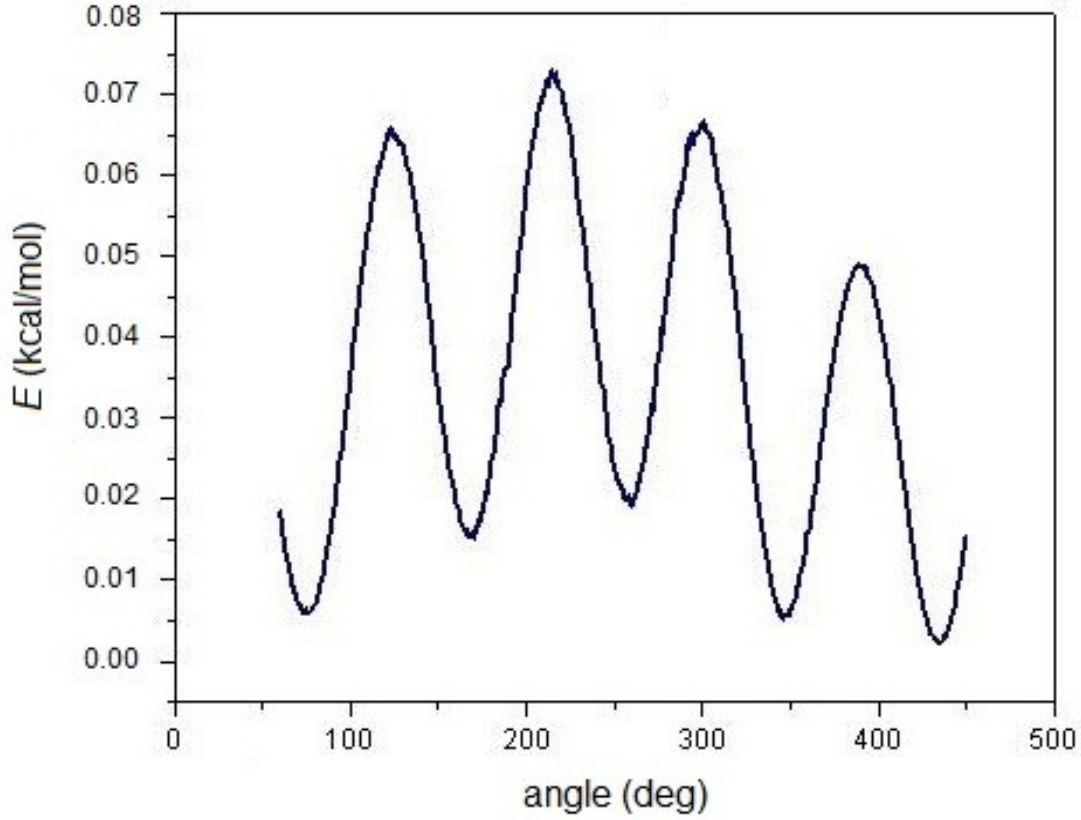

Figure S4. Potential energy for rotation of the propellers **C12a5** and **C12c5**.

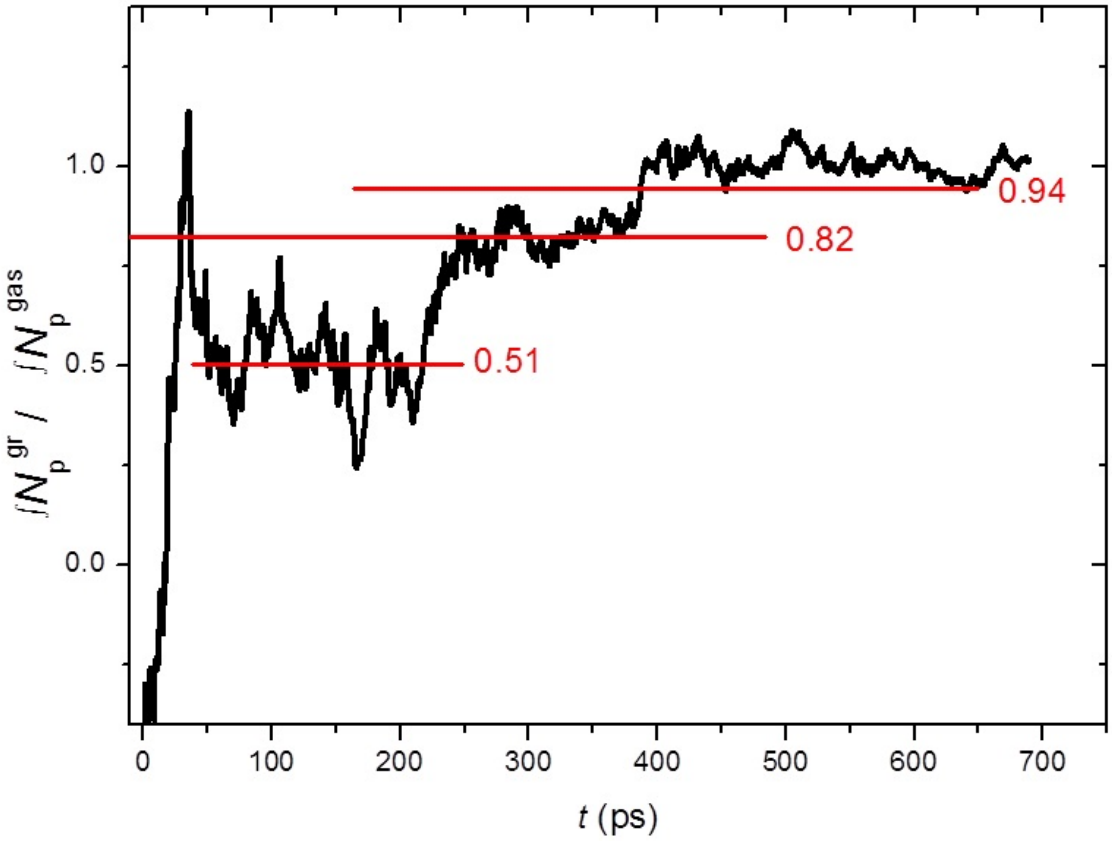

Figure S5. Absolute value of $\int N_p^{gr}/\int N_p^{gas}$ in the molecular rotor **C12a5** driven by gas flow (He, 2250 ms^{-1}, 2 He/nm^3).

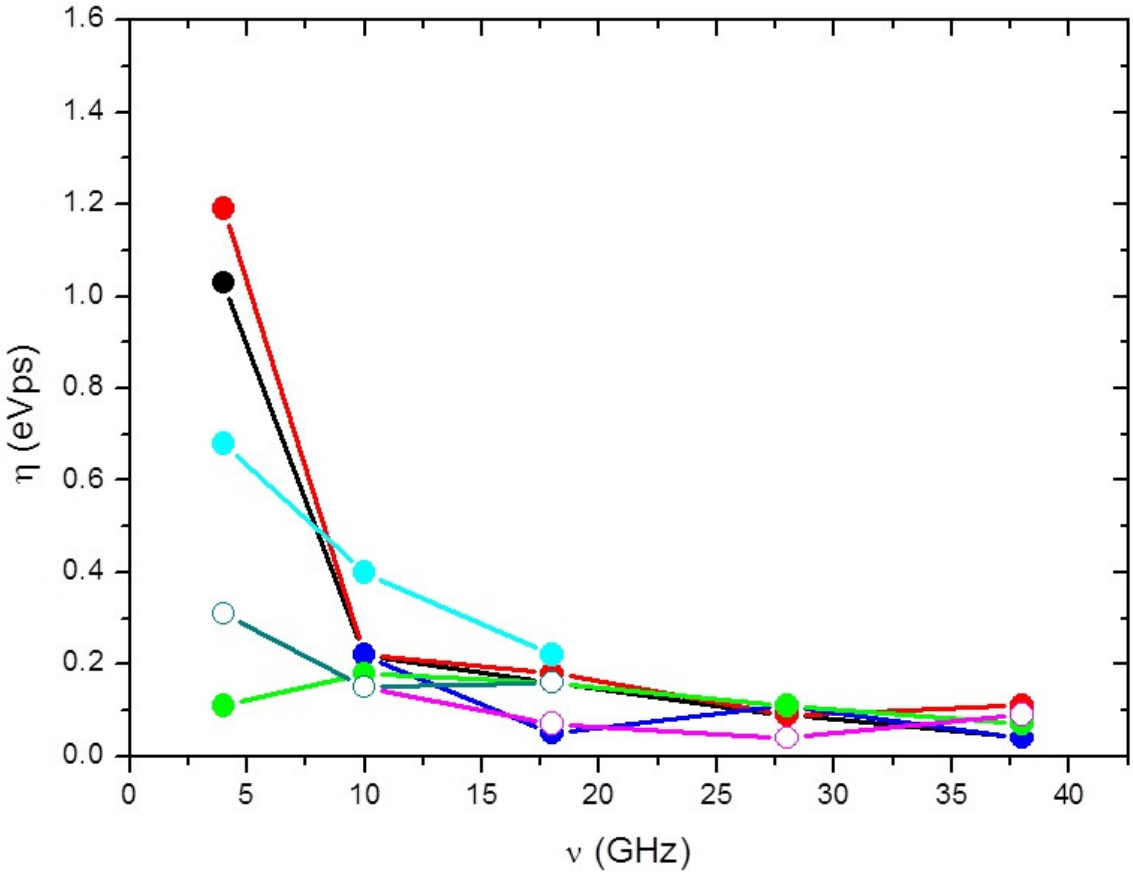

Figure S6. Friction coefficient η^{gas} from $<N_P^{gr}>$ obtained in gas flow, as a function of rotational frequency: η^{gas} **C10a4** –●– ; η^{gas} **C10c4** –●– ; η^{gas} **C12a5** –●– ; η^{gas} **C12c5** –●– ; η^{gas} **C12c5nch** –○– ; η^{gas} **C14a6** –●– ;η^{gas} **C14a6nch** –○– .

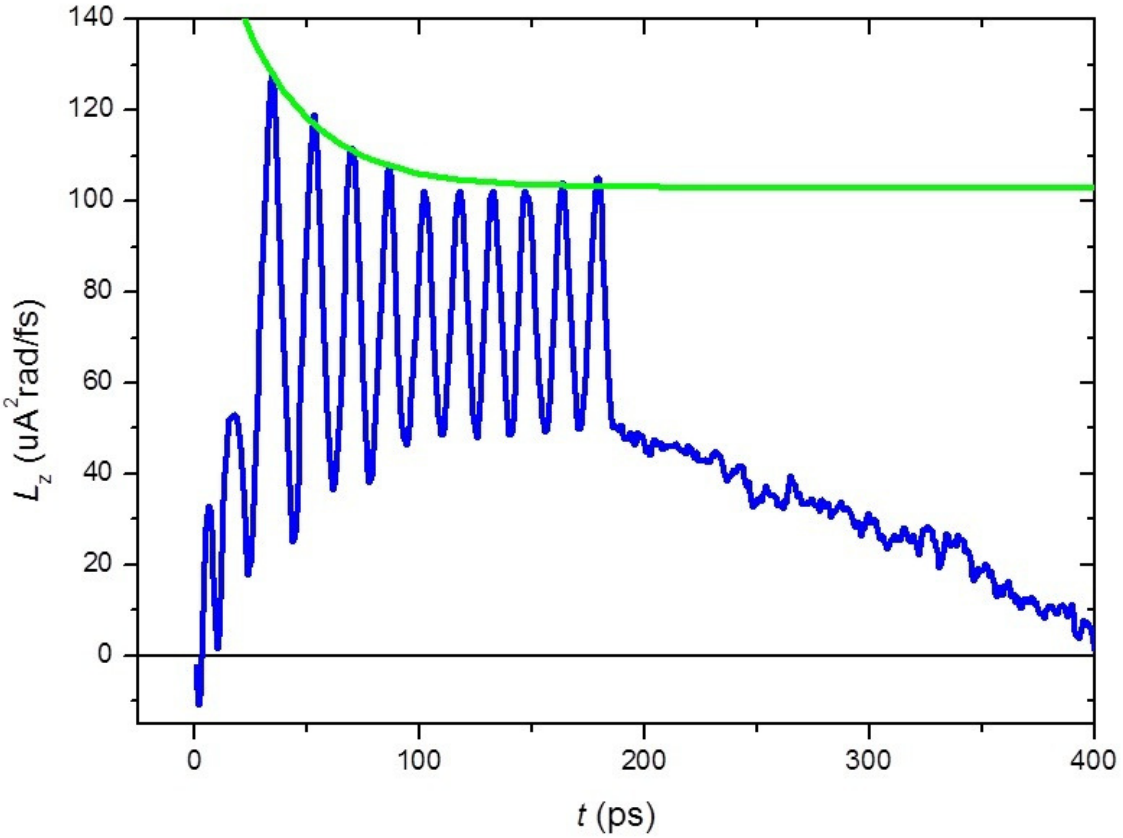

Figure S7. Libration of the propeller in molecular rotor **C14a6** driven by rotating electric field. The field was turned on at $t = 0$ and off at $t = \sim 190$ ps. — L_z of the rotator; — fit to libration decay.

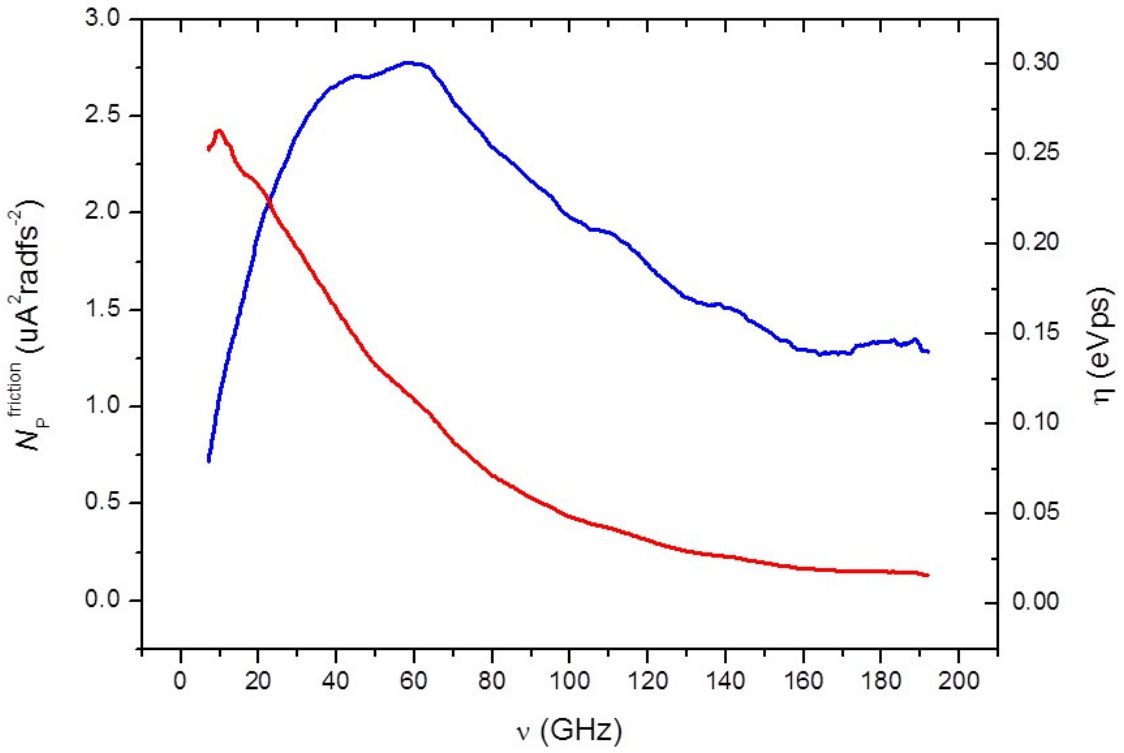

Figure S8. Friction torque $N_p^{friction}$ and friction coefficient η in molecular rotor **C14a6** as a function of rotational frequency. — η^{dec}; — $N_p^{friction}$.

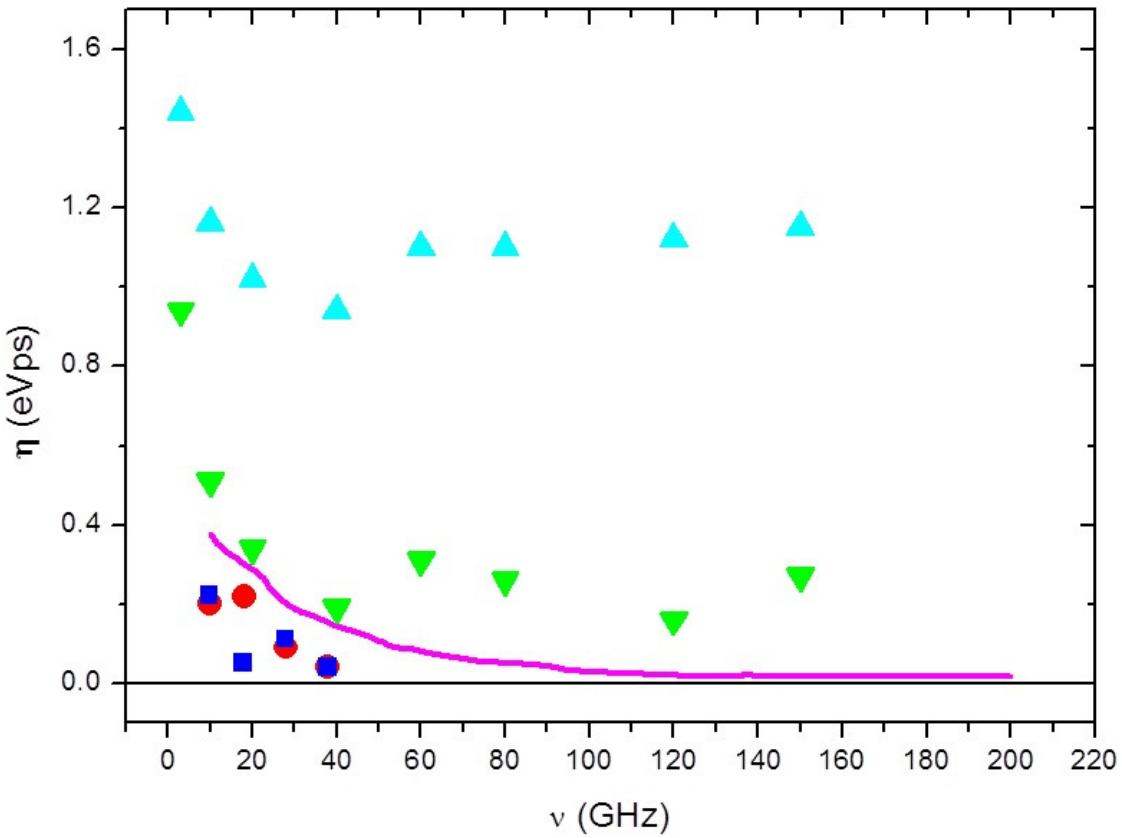

Figure S9. Friction coefficients for the molecular rotor **C12a5**. η_a ▲; η_s ▼; η^{gas} ● ; η^{gas}_{st} ■ ; η^{dec} ——.

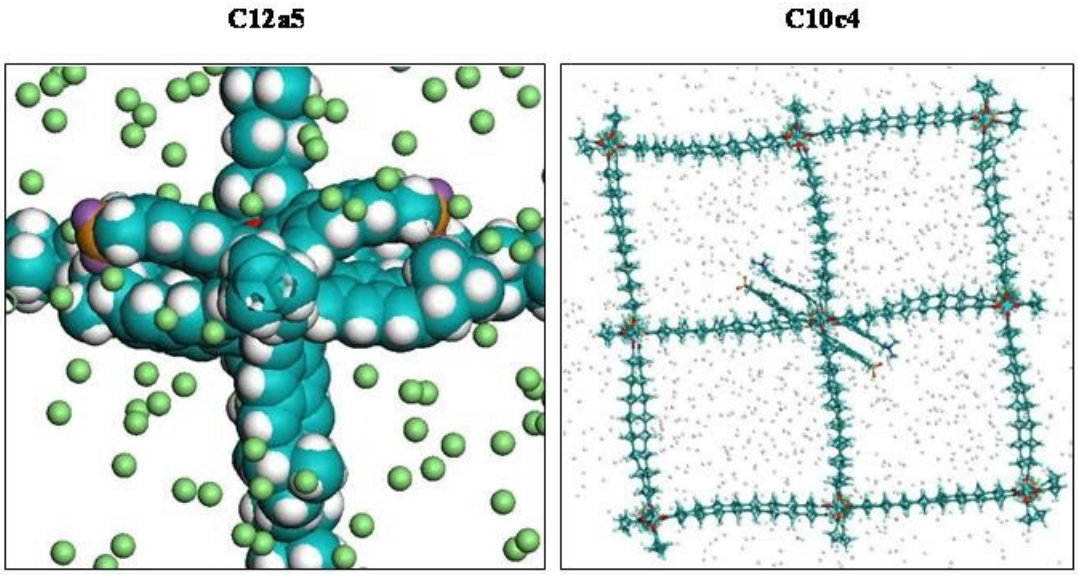

Figure S10. Shape deformations of rotors **C12a5** and **C10c4** in a flow of He gas.

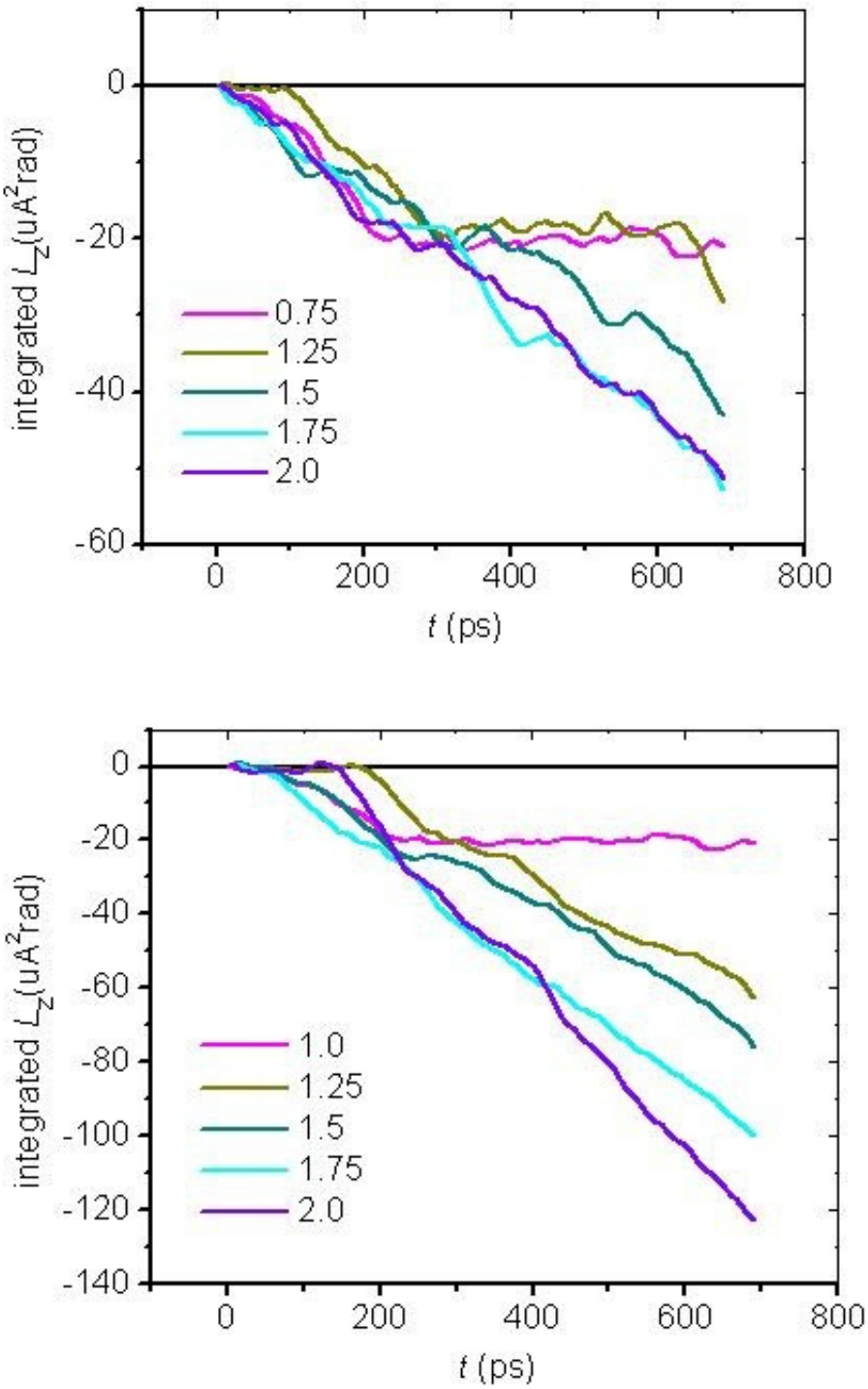

Figure S11. Integrated L_z of propeller **5c** at various He gas atom densities (top, expressed as multiples of the standard density of 2 He/nm^3, keeping velocity constant at 1841 ms^{-1}) and of various He gas atom energies (bottom, expressed as multiples of the energy at standard velocity of 1841 ms^{-1}, keeping density constant at 2 He/nm^3).

Movie File 1 Animation of Molecular Rotor **C12c5**
Movie File 2 Animation of Molecular Rotor **C12c5** in a Stream of He Gas

References

1. Singh, U. C.; Kollman, P. A. *J. Comp. Chem.* **1984**, *5*, 129.
2. Frisch, M. J.; Trucks, G. W.; Schlegel, H. B.; Scuseria, G. E.; Robb, M. A.; Cheeseman, J. R.; Zakrzewski, V. G.; Montgomery Jr., J. A.; Stratmann, R. E.; Burant, J. C.; Dapprich, S.; Millam, J. M.; Daniels, A. D.; Kudin, K. N.; Strain, M. C.; Farkas, O.; Tomasi, J.; Barone, V.; Cossi, M.; Cammi, R.; Mennucci, B.; Pomelli, C.; Adamo, C.; Clifford, S.; Ochterski, J.; Petersson, G. A.; Ayala, P. Y.; Cui, Q.; Morokuma, K.; Salvador, P.; Dannenberg, J. J.; Malick, D. K.; Rabuck, A. D.; Raghavachari, K.; Foresman, J. B.; Cioslowski, J.; Ortiz, J. V.; Baboul, A. G.; Stefanov, B. B.; Liu, G.; Liashenko, A.; Piskorz, P.; Komaromi, I.; Gomperts, R.; Martin, R. L.; Fox, D. J.; Keith, T.; Al-Laham, M. A.; Peng, C. Y.; Nanayakkara, A.; Challacombe, M.; Gill, P. M. W.; Johnson, B.; Chen, W.; Wong, M. W.; Andres, J. L.; Gonzalez, C.; Head-Gordon, M.; Replogle, E. S.; J. A. Pople, Gaussian 98, Revision A.6, Gaussian, Inc., Pittsburgh, PA 1998. www.gaussian.com
3. Rappé, A. K.; Casewit, C. J.; Coldwell, K. S.; Goddard, W. A. III; Skiff, W. M. *J. Am. Chem. Soc.* **1992**, *114*, 10024.
4. Rappé, A. K.; Goddard, W. A. III *J. Phys. Chem.* **1991**, *95*, 3358.
5. Prokop, A.; Vacek, J., unpublished results.
6. Dennis, J. E., Gay, D. M. & Welsch, R. E. *Acm. Trans. Math. Software* **1981**, *7*, 348.